RSC Advances

ROYAL SOCIETY OF CHEMISTRY

www.rsc.org/advances

Journal Name

ARTICLE

Poly(ionic liquid)/ionic liquid/graphene oxide composite quasi solid-state electrolytes for dye sensitized solar cells

Received 00th January 20xx,
Accepted 00th January 20xx

DOI: 10.1039/x0xx00000x

www.rsc.org/

Bencai Lin [a, b*], Tianying Feng [a], Fuqiang Chu [a], Shuai Zhang [a], Ningyi Yuan [a, b], Jianning Ding [a, b, c *]

Poly(ionic liquid)/ionic liquid/graphene oxide (poly(IL)/IL/GO) composite gel electrolytes containing poly(1-butyl-3-vinylimidazolium bis(trifluoromethanesulfonyl) imide), 1-propyl-3-methylimidazolium iodide and graphene oxide are prepared for dye-sensitized solar cells (DSSCs), without any volatile organic solvent. The conductivity of the composite electrolyte is significantly increased by adding a proper amount of GO, and the DSSCs based on composite electrolytes containing GO show higher power conversion efficiency performance and better long-term stability compare to that without GO. The DSSC based on the composite electrolytes which containing 2 wt% of GO show an overall power conversion efficiency of 4.83% under simulated AM 1.5 solar spectrum irradiation. The superior long-term stability of the DSSCs indicates that this type of composite electrolytes could overcome the drawbacks of volatile liquid electrolytes, and offer a feasible method to fabricate DSSCs in future practical applications.

Introduction

Dye-sensitized solar cell (DSSC), a kind of photovoltaic device which could directly convert solar energy into electrical energy without emissions, is attracting a great deal of interest because of its low cost, ease of fabrication and high power conversion efficiency.[1-3] As one of the key components of DSSC, the electrolyte which transfers charge from the counter electrode to the dye has much effect on the energy conversion efficiency and stability of the DSSCs. Recently, power conversion efficiency up to 12.3% have been achieved for DSSC using a liquid organic electrolyte.[4] However, the presence of the organic solvents substantially shorten the working life and affect the practical application of DSSC because of the evaporation and leakage of organic solvents. To overcome these problems of DSSC, p-type inorganic semiconductor,[5, 6] inorganic hole transportation materials [7-9] and polymer-based gel electrolytes [10-14] were prepared to substitute for the organic solvents-based electrolytes. Among these technologies, the polymers-based quasi-solid-state electrolytes have been attracting much attention due to their nonflammability, negligible vapor pressure, and good contact with the nanocrystalline TiO_2 electrode and counter electrode.[15]

Ionic liquid (IL) had attracted much attention for its unique properties such as negligible vapor pressure, excellent thermal stability, broad electrochemical potential window and high ionic conductivity. These unique properties make IL very appealing materials as stable and safe electrolyte media in lithium batteries,[16] high-temperature proton exchange membrane fuel cells, [17,18] and alkaline anion exchange membrane fuel cells.[19] Recently, much work has been done to develop DSSCs with IL-based electrolytes.[20-22] The evaporation problem of the traditional organic solvent based electrolytes can be solved by using IL as electrolyte. [15] Recently, we prepared the DSSCs with IL/IL-tethered graphene oxide composite electrolytes which showed an overall power conversion efficiency of 7.04% under simulated AM 1.5 solar spectrum irradiation at 100 mW cm^{-2}.[23]

As a new class of polymers, poly(ionic liquid) (poly(IL)) which combine both the properties of ionic liquid and polymers have attracted much attention in recent years. Poly(IL) was successfully used for quasi-solid-state DSSCs, and the devices showed high power conversion efficiency and excellent long-term stability.[24, 25] It is reported that addition of inorganic nanoparticles into the electrolytes is an effective way to improve the DSSC performance.[26] Lin et. al prepared DSSCs with poly(ether urethane)/poly(ethylene oxide)-modified SiO_2 based electrolytes, and the devices showed a power conversion efficiency of 4.86%.[27] The efficiency of DSSCs has been significantly increased by addition of small amounts of graphene sheets into IL-based electrolytes reported by Brennan. et al.[28] In general, the uniformly dispersed nanomaterials in electrolytes could bring beneficial contributions to the short circuit current density (J_{sc}) and long-term stability of the devices.[24, 26, 27] However, the aggregation of inorganic nanomaterials in electrolyte was commonly observed.[26] Proper surface modification could enhance the compatibility of inorganic nanomaterials and the ionic liquids in the preparation of the corresponding electrolyte for DSSCs.[25] Graphene oxide

[a] School of Materials Science and Engineering, Jiangsu Collaborative Innovation Center for Photovolatic Science and Engineering, Changzhou University, Changzhou, 213164, Jiangsu, China, E-mail: linbencai@cczu.edu.cn; dingjn@cczu.edu.cn
[b] Jiangsu Province Cultivation base for State Key Laboratory of Photovoltaic Science and Technology, Changzhou University, Changzhou, 213164, Jiangsu, China
[c] Micro/Nano Science and Technology Center, Jiangsu University, Zhenjiang, 212013, China

(GO) has much oxygen-containing functional groups such as hydroxyl, carboxylic acid, and can be easily chemical modification.[29-31] In our previous work, the DSSCs based on ionic liquid-tethered graphene oxide (IL-GO)/ionic liquid electrolytes were fabricated.[23] The introduced of IL-GO into IL-based electrolyte is a successful method to improve the performance of DSSCs. However, the devices with liquid state electrolyte were still suffering leakage problems in the practical use, and the long-term stability of the DSSCs should be further enhanced. In addition, the preparation of IL-GO is not a simple process.

Here, we report the fabrication of high performance DSSCs using poly(IL)/IL/GO composite gel electrolyte as a replacement for traditional organic solvent based gel electrolytes. The influence of GO content on the DSSC properties was systematically investigated. The GO could be well dispersed in poly(IL)/IL to form quasi-solid-state gel electrolytes, without using any volatile organic solvents. The fabricated quasi solid-state DSSCs with GO show better performance and stability than that without GO gel electrolytes, which indicating the poly(IL)/IL/GO composite gel electrolytes are a promising candidate for DSSCs with good durability.

Experimental

Materials

TiO_2 nanoparticles (Titanium (IV) oxide, T-20nm), H_2PtCl_6 and iodine were obtained from Sigma-Aldrich. Flaky graphite powder (45 μm , Qingdao Huatai Lubricant Sealing S&T China), sulfuric acid, potassium hydroxide, ethyl acetate, 1-iodopropane, 1-methylimidazole, 3-bromopropylamine hydrobromide and 4-tert-butylpyridine (TBP) were purchased from Aladdin. Lithiumbis (trifluoromethanesulfonyl) imide (LiTFSI) were purchased from Alfa Aesar and used as received. N719 dye，Surlyn (ionomer films of 25-μm thick) and FTO conducting glass (resistance of 25 Ω/square, transmittance of 85 %) were purchased from Dalian Rainbow Solar Technology Development Co Ltd., Dalian, China. All reagents were of analytical grade and were used as received unless otherwise stated.

Synthesis of 1-propyl-3-methylimidazolium iodide (PMII)

PMII was synthesized as follows: [32] 8.5 g (0.05 mol) 1-iodopropane was dissolved in 20 ml ethyl acetate, 4.1 g (0.05 mol)1-methylimidazole was then added and the mixture was stirred for 2 h at 0 °C. The reaction bath was heated to room temperature and then stirred for another 48 h. The resultant viscous oil was washed with ethyl ether three times, and then dried in dynamic vacuum at 80 °C for 24 h. ^{1}H NMR (400 MHz, D_2O): δ: 8.64 (S, 1H), 7.39 (S, 1H), 7.34 (S, 1H), 4.07 (t, 2H), 3.80 (S, 1H), 1.82 (m, 2H) , 0.83 (m, 3H).

Synthesis of poly(1-butyl-3-vinylimidazolium bis(trifluoromethanesulfonyl) imide) ([PBVIm][TFSI], poly(IL)

Poly(IL) was synthesized according to the previous report: [24] 1-butyl-3-vinylimidazolium bromide ([BVIm][Br]) was firstly synthesized from 1-bromobutane and 1-vinylimidazole under a nitrogen atmosphere using a magnet stirred in an ice water bath for 3 days. The resultant viscous oil was washed with ethyl ether three times. ^{1}HNMR: (400 MHz, $CDCl_3$): 10.98 (s, 1H), 7.77 (s, 1H), 7.50 (dd, 1H), 7.46 (m, 1H), 5.95(m, 1H), 5.36 (m, 1H), 4.38 (t, 3H), 1.91(m, 2H), 1.37(m, 2H), 0.96 (t, 3H). Yield: 88%. Poly(1-butyl-3-vinylimidazolium bromide was prepared via free radical polymerization of 1-butyl-3-vinylimidazolium bromide in ethanol at 60 °C under a nitrogen atmosphere for 24 h. Poly(1-butyl-3-vinylimidazolium bis(trifluoromethanesulf-onyl) imide) was abtained by anion-exchange of [PBVIm][Br] with LiTFSI in aqueous solution.

Preparation of graphene oxide (GO)

Graphene oxide (GO) was obtained from the graphite powder following previous work. [33, 34] Typically, 1.00 g of graphite, 0.50 g of $NaNO_3$ and 23 mL of H_2SO_4 (98%) was added into a 100 mL flask, and then the mixture was stirred for 15 min in an ice bath. Then 3.00 g $KMnO_4$ was added and the mixture was stirred at 35°C for 30 min, followed 46 mL of deionized water was added into the mixture and stirred at room temperature for 30 min. Then, 10 mL of 30% H_2O_2 was added into the mixture, and finally cooled down to room temperature. The obtained precipitated was washed with 5% HCl and H_2O several times before being dried under vacuum.

Preparation of poly(IL)/IL/GO electrolytes

The liquid electrolyte was composed of 1M PMII, 0.1M I_2, 0.2M LITFSI, 0.5M TBP, 20 wt% of the poly(IL) (based on the weight of the liquid electrolyte) and different amount of GO was added into the liquid electrolyte and stirred at 60 °C for 6 h, then the homogeneous poly(IL)/IL/GO electrolytes were obtained.

Fabrication of DSSCs

The DSSCs were fabricated by using a conventional process according to the previous report:[35,36] TiO_2 working electrodes were prepared on the cleaned FTO coated glass substrates, the FTO glasses were sticky with adhesive tape on both parallel edges to control the thickness of the TiO_2 films, and were annealed at 500 °C for 30 min to ensure good electrical contact between the TiO_2 films and the FTO substrates. Dye adsorption was carried out by immersing the TiO_2 working electrodes in N719 dye solution (0.5 mM in ethanol) at room temperature for 24 h，then the TiO_2 electrodes were rinsed with ethanol and dried under nitrogen flow. The Pt counter electrode was prepared by dripping a drop of 10 mM H_2PtCl_6 ethanol solution placed onto FTO glass substrate, followed by annealed at 450 °C for 30 min. DSSCs were fabricated by sandwiching poly(IL)/IL/GO electrolytes between dye-sensitized TiO_2 working electrode and Pt counter electrode, which were using a sheet of a thermoplastic frame (25-μm thick, Surlyn) as a spacer between the two electrodes. The typical active area of the cell was 0.2025 cm^2.

Characterization techniques and instrumental

XRD analysis was carried out using a RAD-3X (Rigaku Corporation, Tokyo, Japan) diffractometer with Cu-Kα radiation. AFM images were recorded using Agilent AFM with Pico plus molecular imaging system in the non-contact mode. The conductivity of the electrolytes was characterized in an

ordinary cell composed of Teflon tube and two identical stainless steel electrodes (diameter of 1 cm) on a CHI660c electrochemical workstation at room temperature, using the AC impedance method over the frequency range 0.1 Hz-1M Hz.[24] Steady-state voltammetry was tested in a conventional photo electrochemical cell equipped with a radius of 5.0 μm platinum ultramicroelectrode (CHI107) as the working electrode, and a platinum foil as a counter electrode and reference electrode, respectively.[10] The current-voltage (*J-V*) characteristics were examined by a Keithley model 2400 source meter (Keithley Instruments, Inc. Cleveland, USA) under AM 1.5 solar spectrum irradiation of 100mW/cm^{-2}. Electrochemical impedance spectra (EIS) were conducted using a Zahner IM6ex electrochemical workstation. A perturbation of 10 mV was applied, and the frequency ranged from 0.1 Hz to 1M Hz. Cyclic voltammetry (CV) tests were carried out using a computer-controlled potentiostat (Autolab Type III) by a polished platinum electrode vs a saturated KCl calomel reference electrode from –0.7 to 1.2 V at an ambient atmosphere, and the scan rates is 75 mV·s^{-1}). Intensity-modulated photocurrent spectroscopy (IMPS) and photovoltage spectroscopy (IMVS) were measured on a controlled intensity modulated photo spectroscopy (Zahner Co., Kansas City, MO, USA) in ambient conditions under illumination through the FTO glass side, using a blue light-emitting diode as the light source (BLL01, λmax = 470 nm, spectral half-width = 25 nm; Zahner Co.) driven by a frequency response analyzer, and the light intensity (incident photon flux) of the DC component was controlled at 2.5 × 10^{16} cm^{-2}s^{-1}. During the IMVS and IMPS measurements, the cell was illuminated with sinusoidally modulated light having a small AC component (10 % or less of the DC component).

Results and discussion

Characterization of electrolytes

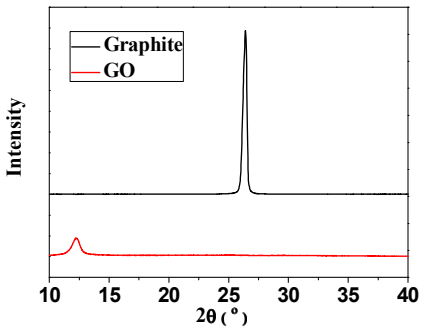

Fig. 1 XRD spectra of graphite and GO.

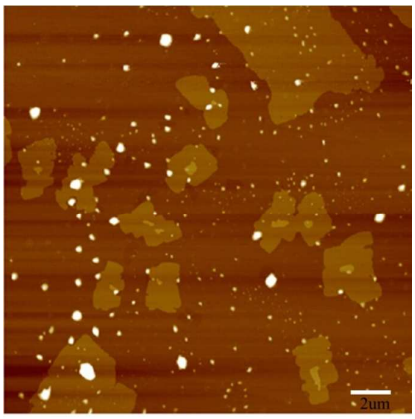

Fig. 2 The AFM image of GO.

It has been demonstrated that it is difficult to disperse inorganic nanomaterials into common organic solvent due to the lack of surface-functional groups.[26] In this work, graphene oxide (GO) was prepared and applied as the additive for the preparation of IL-based quasi solid-state electrolyte for DSSCs. In the present work, GO was prepared following the Hummers method.[33,34] Poly(IL) and IL were obtained according to the previous reports.[15, 24] The purity and chemical structure of the synthesized IL was confirmed by ^{1}H NMR measurements (see Experimental Section). X-Ray diffraction (XRD) measurements were used to investigate the structure of GO. The XRD spectra of graphite and GO are shown in Fig. 1. It can be clearly seen that an intense (002) diffraction peak of graphite appears at 26.4°, and the interlay space is 0.34 nm, while the (001) diffraction peak of GO appears at 12.2° and the interlay space is 0.73 nm. The increase of interlayer distance of GO was caused by the intercalation oxygenated functional groups on the surface of graphite nano-sheet. The atomic force microscope (AFM) measurements were used to confirm the morphology of GO, and the results indicating GO nano-sheets were obtained (Fig. 2).

IL-based quasi-solid-state electrolytes containing various content of GO were prepared and coded as electrolyte A-F: (A) 0 wt% GO, (B) 1.0 wt% GO, (C) 1.5 wt% GO, (D) 2.0 wt% GO, (E) 2.5 wt% GO, (F) 2.5 wt% GO. The DSSCs based on electrolyte A-F are denoted as cell A-F, respectively. All the electrolytes are quasi-solid-state gels at room temperature. The performance of a DSSC is usually influenced by the conductivity of electrolyte. The conductivities of electrolytes containing different content of GO were measured with a CHI660c electrochemical workstation at room temperature, and the results listed in Table 1. It can be clearly seen that the conductivities of the composite electrolytes increases with the incorporation of proper amount of GO. For example, the conductivity of electrolyte A is 5.54 × 10^{-4} S cm^{-1}, and it reaches to the maximum value of 7.82 × 10^{-4} S cm^{-1} by the electrolyte D which contains 2.0 wt% of GO. The addition of GO favors the formation of ion transportation network in the quasi solid-state electrolyte, which improved the movement of

Table 1 Photovoltaic performance parameters of the DSSCs based on electrolytes A-F measured under AM 1.5 solar spectrum irradiation of 100mW cm^{-2}.

Cell	GO (wt.%)	Conductivity (10^{-4} S cm^{-1})	J_{sc} (mA cm^{-2})	V_{oc} (Mv)	FF	η (%)
A	0	5.54	3.34	0.60	0.72	1.46
B	1.0	6.72	4.07	0.70	0.75	2.16
C	1.5	7.45	7.42	0.71	0.75	3.85
D	2.0	7.82	8.84	0.72	0.76	4.83
E	2.5	6.54	5.59	0.69	0.75	2.90
F	3.0	6.06	3.47	0.68	0.73	1.73

free ions in a regular direction.[37, 38] However, the excess GO result in the decrease of the conductivity of the quasi solid-state electrolyte, indicating potential saturation of ion transport channels formed by the incorporation of GO, and the further addition of GO could block the formed ion transport channels.[31] Therefore, it is not surprising that excess GO resulted in low ionic conductivity.

Cyclic voltammetry (CV) was tested to investigate the effect of GO content on the redox activity of the IL-based electrolytes. The CV curves of the I^-/I_3^- system with different content GO were measured by a polished platinum electrode vs a saturated KCl calomel reference electrode from –0.7 to 1.2 V, and the results were showed in Fig. 3. There are two redox waves can be seen in Fig. 3, the left one which is located at lower potential corresponds to the redox reaction of $I_3^- + 2e^- \leftrightarrow 3I^-$, and the other one corresponds to the redox reaction of $3I_2 + 2e^- \leftrightarrow 2I_3^-$. In general, the higher peak current density of the CV curves means that the reaction kinetics is more active.[39] The values of peak current density increase with increasing the content of GO from 0 to 2.0 wt%. These results indicating that the GO is acting as a catalyst for the redox reaction in the gel electrolytes and allows for an increase in current density. However, the values of peak current density decreases with a further addition of GO. As mentioned before, the further addition of GO could block the ion transport channels formed in the gel electrolytes which resulted in low current density.

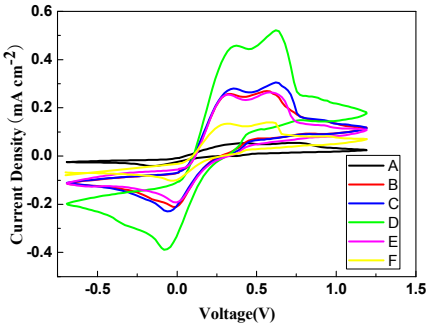

Fig. 3 CV curves of electrolyte A-F.

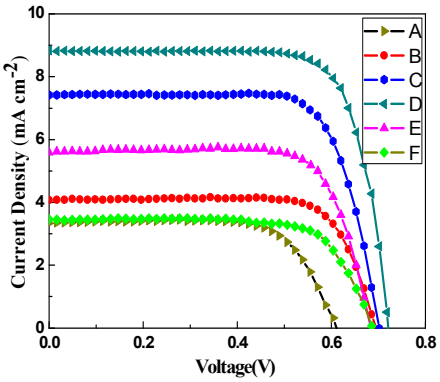

Fig. 4 The J-V curves of DSSCs assembled with electrolytes A-F under simulated AM 1.5 solar spectrum irradiation at 100 mW cm^{-2}. The devices are tested with an aluminum foil mask with an aperture area of 0.1 cm^2.

Characterization of DSSCs

Fig. 4 shows the photocurrent density-voltage characteristics of DSSCs based on electrolytes A-F containing different content of GO, which were measured under AM 1.5 solar spectrum irradiation of 100 mW cm^{-2}. The data of the open circuit voltage (V_{oc}), short circuit current density (J_{sc}), fill factor (FF) and the photoelectric conversion efficiency (η) are also summarized and listed in Table 1. It can be seen that the DSSC based on electrolyte A without GO shows a J_{sc} of 3.34 mA cm^{-2}, V_{oc} of 0.60 mV, FF of 0.72, and η of 1.46%, respectively. By increasing the content of GO to 2.0 wt%, the maximum values of Jsc, Voc and η are obtained, but these values decrease with additional GO. The DSSC based on electrolyte D which containing 2.0 wt% GO shows the best performance, and shows a maximum photoelectric conversion efficiency of 4.83%. Unfortunately, with the excess addition of GO into the IL-based gel electrolyte, the performance of the devices decrease probably due to the high viscosity of the gel electrolyte and the aggregation of GO which blocked the charge transfer in the gel electrolyte.

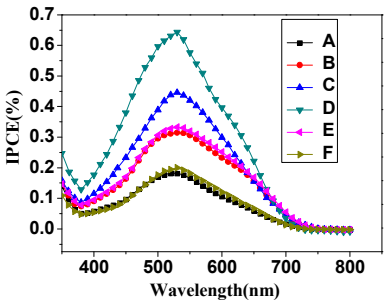

Fig. 5 The IPCE curves of DSSCs based on different gel electrolytes.

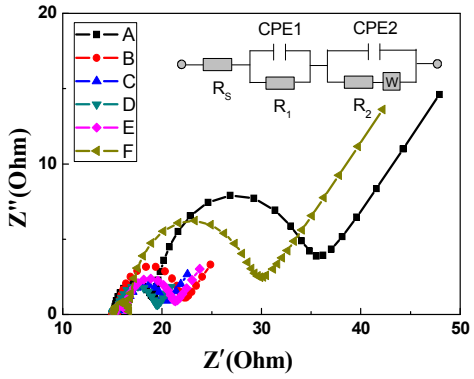

Fig. 6 EIS Nyquist plots of cell A-F.

Table 2 Electrochemical impedance spectroscopy results of Cell A-F.

Cell	R_1/Ω	R_2/Ω	R_{diff}/Ω
A	15.20	14.24	39.13
B	10.03	6.02	15.41
C	7.47	3.61	10.10
D	5.97	3.52	5.04
E	8.82	4.45	11.07
F	10.68	8.93	30.92

The incident photo-to-current conversion efficiency (IPCE) curves of cell A-F are shown in Fig. 5. The maximum IPCE value as high as 64.3% at 530 nm was obtained for Cell D, which is higher than that of Cell A (18.2%), Cell B (31.1%), Cell C (44.6%), Cell E (33.3%), and Cell F (20.1%), respectively. The IPCE values are consistent with the photoelectric conversion efficiency of the DSSCs.

The kinetics of electrochemical and photo-electrochemical processes of DSSCs, such as the electronic and ionic processes occurring in DSSCs were investigated by the electrochemical impedance spectroscopy (EIS) technique. Fig. 6 shows the EIS Nyquist plot of cells A-F which measured at -0.7V bias under dark environment. Generally, three semicircles can be seen in the EIS spectra of DSSCs. As shown in Fig. 6, from high to low frequency, the three semicircles correspond to the charge transfer resistance at the counter electrode (R_1), the resistance of TiO_2/FTO, TiO_2/electrolyte interface (R_2), and the Warburg diffusion process (R_{diff}) of I^-/I_3^- in the electrolyte, respectively.[40-42] The overall series resistance was coded as R_s as shown in Fig. 6. The corresponding fitting values of the resistance showed in Fig. 6 are listed in Table 2. By increasing the content of GO to 2.0 wt%, the maximum values of R_1 was obtained, but the value decrease with additional GO. This phenomenon is in good coordination with the reversed order observed for the η of the DSSCs. The trends of R_2 *and* R_{diff} are similar with R_1, and cell D with 2 wt% GO shows the minimum resistance values of 3.52 and 5.04 Ω. These results supports that the addition of proper content of GO could enhances the charge transport at the TiO_2/electrolyte interface, as well as the enhancement of transport of I^-/I_3^- ions in the electrolyte.[43]

Intensity-modulated photocurrent spectroscopy (IMPS) and photovoltage spectroscopy (IMVS) measurements were conducted to further investigate the GO content effect on the electron transport and charge recombination in the DSSCs, and the IMPS (Fig. 7A) and IMVS (Fig. 7B) plots of Cell A-F are shown in Fig. 7. The transit time (τ_d) and electron lifetime (τ_n) can be calculated using the follow equations:

$$\tau_d=(2\pi f_{min}(\text{IMPS}))^{-1}$$
$$\tau_n=(2\pi f_{min}(\text{IMVS}))^{-1}$$

where f_{min}(IMPS) and f_{min}(IMVS) are the frequencies at the minimum imaginary component in the IMPS and IMVS plots.[23] Table 3 lists the electron lifetime and transit time of cells A-F. Cell D shows the longest electron lifetime of 96.89 ms and the shortest transit time of 1.89 ms among the devices. A long τ_n favors the collection of electrons before they recombine in the cells,[44] and indicating more electrons surviving from the back reaction which results in high photocurrent.[23,45] The τ_d is much shorter than τ_n, and this is important for DSSCs to collect the charge injected by dye.[46] Both the tendencies of τ_n and τ_d are in good agreement with the fact that the performance of DSSCs is improved by increasing the content of GO until it reaches 2 wt%. Compared with Cell A, the electron lifetime of DSSCs based on composite gel electrolytes containing GO are enough to favors electron transport through a longer distance with less diffusive hindrance, and finally leads to enhanced photoelectric conversion efficiency.[47]

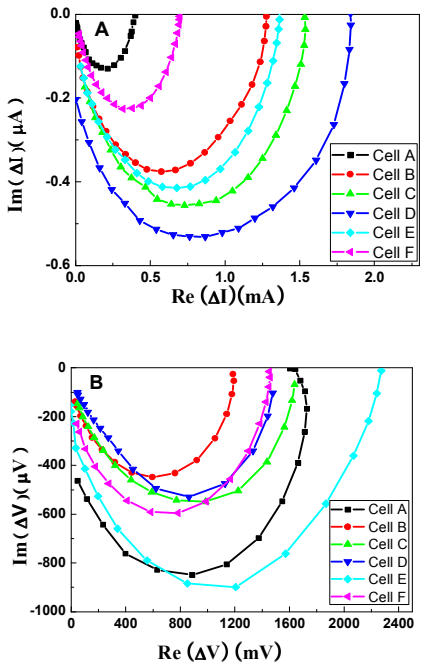

Fig. 7 IMPS (A) and IMVS (B) plots of cell A-F.

Table 3 Detailed IMPS/IMVS parameters of cell A-F.

Cell	$f_{min(IMPS)}$ (Hz)	$f_{min(IMVS)}$	τ_d (ms)	τ_n (ms)
A	17.1	24.56	9.31	6.48
B	34.44	7.58	4.62	21.01
C	63.71	2.88	2.50	55.37
D	84.48	1.64	1.89	96.89
E	47.28	4.78	3.37	33.35
F	24.56	11.57	6.48	13.76

The long-term stability of DSSCs is still a challenge for their practical applications. Here, the long-term stability of DSSCs was investigated via an accelerating aging test of the sealed devices.[48] The total efficiencies of Cell A, D and F are normalized to the values measured on the first day, as shown in Fig. 8. The efficiency of all the three devices was enhanced at the early stage of long-term stability testing due to the increased of the dye regeneration rate which enhanced the J_{sc} of DSSCs.[47,49] As shown in Fig. 8, Cell D and Cell F retains 97% and 91% of their initial efficiency after 1200 h, while Cell A only maintained 85% of the initial efficiency under the same conditions. The long-term stability of DSSCs is greatly improved by addition of GO probably due to the gel network hindered the leakage of the ionic liquid of the electrolyte effectively. In addition, the nanomaterial is effective in preventing the release of ionic liquid component from the composite electrolyte.[18] Compared with that of Cell D, Cell F showed a lower long-term stability probably due to the aggregation of GO in the electrolyte.[24] All these results demonstrating that DSSCs based on this type of gel electrolyte containing proper content of GO have excellent practical stability.

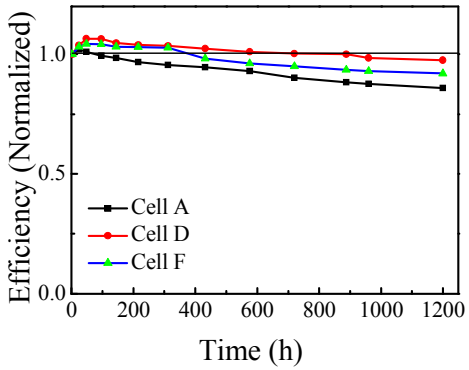

Fig. 8 Time-course variation of the normalized efficiency for the DSSCs during accelerated aging tests at 60 °C.

Conclusions

In summary, poly(IL)/IL/GO composite gel electrolyte have been prepared for quasi-solid state DSSCs. The conductivity of the composite electrolytes was increased by incorporating of proper content of GO. Compared with the DSSC based on electrolyte without GO, the DSSCs based on composite electrolyte with proper GO show higher open circuit voltage, short circuit current density, photoelectric conversion efficiency, and better long-term stability. The DSSC based on composite electrolyte with 2 wt% of GO showed maximum efficiency of 4.83 % under AM 1.5 solar spectrum irradiation. The composite IL-based gel electrolytes prepared in the present work could overcome the leakage problem of liquid electrolytes based DSSCs and demonstrate a feasible approach for the practical applications of quasi-solid-state DSSCs.

Acknowledgements

This work was supported by National Natural Science Foundation of China (No. 51303017 and 21476031), the Natural Science Foundation of the Jiangsu Higher Education Institutions of China (Grant No. 13KJB150003), and a Project Funded by the Priority Academic Program Development of Jiangsu Higher Education Institutions.

Notes and references

1 M. Gratzel, R. A. J. Janssen, D. B. Mitzi and E. H. Sargent, *Nature,* 2012, **488**, 304–312.
2 A. F. Nogueira, J. R. Durrant and M. A. De Paoli, *Adv Mater*, 2001, **13**, 826-830.
3 A. Hagfeldt, G. Boschloo, L. Sun, L. Kloo and H. Pettersson, *Chem Rev.* 2010, **110**, 6595−6663.
4 A. Yella, H.-W. Lee, H. N. Tsao, C. Yi, A. K. Chandiran, M. K. Nazeeruddin, E. W.-G. Diau, C.-Y. Yeh, S. M. Zakeeruddin and M. Grätzel, *Science*, 2011, **334**, 629-634.
5 G. Kumara, A. Konno, K. Shiratsuchi, J. Tsukahara and K. Tennakone, *Chem Mater,* 2002, **14**, 954−955.
6 K. Tennakone, G. Senadeera, D. De Silva and I. Kottegoda, *Appl Phys Lett,* 2000, **77**, 2367−2369.
7 C. S. Karthikeyan, H. Wietasch and M. Thelakkat, *Adv Mater,* 2007, **19**, 1091−1095.
8 U. Bach, D. Lupo, P. Comte, J. Moser, F. Weissörtel, J. Salbeck, H. Spreitzer and M. Grätzel, *Nature*, 1998, **395**, 583-585.
9 A. Sepehrifard, B. A. Kamino, T. P. Bender and S. Morin, *ACS Appl Mater Interfaces,* 2012, **4**, 6211−6215.
10 M. Wang, X. Pan, X. Fang, L. Guo, C. Zhang, Y. Huang, Z. Huo and S. Dai, *J Power Sources,* 2011, **196**, 5784–5791.
11 C. Wu, L. Jia, S. Guo, S. Han, B. Chi, J. Pu and L. Jian, *ACS Appl Mater Interfaces,* 2013, **5**, 7886−7892.
12 Y. Yang, C. Zhou, S. Xu, H. Hu, B. Chen, J. Zhang, S. Wu, W. Liu and X. Zhao, *J Power Sources*, 2008, **185**, 1492–1498.
13 S. K. Ahn, T. Ban, P. Sakthivel, J. W. Lee, Y.-S. Gal, J.- K. Lee, M.-R. Kim and S.-H. Jin, *ACS Appl Mater Interfaces,* 2012, **4**, 2096−2100.

14 Y. Shi, K. Wang, Y. Du, H. Zhang, J. Gu, C. Zhu, L. Wang, W. Guo, A. Hagfeldt, N. Wang and T. Ma, *Adv Mater,* 2013, **25**, 4413–4419.
15 J. Zhao, X. Shen, F. Yan, L. Qiu, S. Lee and B. Sun, *J Mater Chem,* 2011, **21**, 7326-7330.
16 H. Matsumoto, H. Sakaebe and K. Tatsumi, *J Power Sources,* 2006, **160**, 1308-1313.
17 F. Yan, S. Yu, X. Zhang, L. Qiu, F. Chu, J. You and J. Lu, *Chem Mater*, 2009, **21**, 1480-1484.
18 B. Lin, S. Cheng, L. Qiu, F. Yan, S. Shang and J. Lu, *Chem Mater*, 2010, **22**, 1807-1813.
19 M. Guo, J. Fang, H. Xu, W. Li, X. Lu, C. Lan and K. Li, *Journal of Membrane Science*, 2010, **362**, 97-104.
20 W. Xu and C. A. Angell, *Science*, 2003, **302**, 422-425.
21 P. Wang, B. Wenger, R. Humphry-Baker, J.-E. Moser, J. Teuscher, W. Kantlehner, J. Mezger, E. V. Stoyanov, S. M. Zakeeruddin and M. Grätzel, *J Am Chem Soc*, 2005, **127**, 6850-6856.
22 D. Kuang, P. Wang, S. Ito, S. M. Zakeeruddin and M. Grätzel, *J Am Chem Soc*, 2006, **128**, 7732-7733.
23 B. Lin, H. Shang, F. Chu, Y. Ren, N. Yuan, B. Jia, S. Zhang, Y. Wei, X. Yu and J. Ding, *Electrochimica Acta,* 2014, **134**, 209–214.
24 X. Chen, Q. Li, J. Zhao, L. Qiu, Y. Zhang, B. Sun and F. Yan, *J Power Sources*, 2012, **207**, 216-221.
25 G. Wang, L. Wang, S. Zhuo, S. Fang and Y. Lin, *Chem Commun* 2011, **47**, 2700–2702.
26 Y. Zhang, J. Zhao, B. Sun, X. Chen, Q. Li, L. Qiu and F. Yan, *Electrochim Acta*, 2012, **61**, 185-190.
27 Y. Zhou, W. Xiang, S. Chen, S. Fang, X. Zhou, J. Zhang and Y. Lin, *Chem Commun*, 2009, 3895-3897.
28 L. J. Brennan, S. T. Barwich, A. Satti, A. Faure and Y. K. Gun'ko, *J Mater Chem A*, 2013, **1**, 8379-8384.
29 H.-K. Jeong, Y. P. Lee, R. J. Lahaye, M.-H. Park, K. H. An, I. J. Kim, C.-W. Yang, C. Y. Park, R. S. Ruoff and Y. H. Lee, *J Am Chem Soc*, 2008, **130**, 1362-1366.
30 A. Lerf, H. He, M. Forster and J. Klinowski, *The Journal of Physical Chemistry B*, 1998, **102**, 4477-4482.
31 C. Y. Neo and J. Ouyang, *Carbon*, 2013, **54**, 48-57.
32 P. Bonhote, A.-P. Dias, N. Papageorgiou, K. Kalyanasundaram and M. Grätzel, *Inorg Chem*, 1996, **35**, 1168-1178.
33 C. H. Lu, H. H. Yang, C. L. Zhu, X. Chen and G. N. Chen, *Angewandte Chemie*, 2009, **121**, 4879-4881.
34 M. Hirata, T. Gotou, S. Horiuchi, M. Fujiwara and M. Ohba, *Carbon*, 2004, **42,** 2929-2937.
35 S. Ito, P. Chen, P. Comte, M. K. Nazeeruddin, P. Liska, P. Péchy and M. Grätzel, *Progress in photovoltaics: research and applications*, 2007, **15**, 603-612.
36 S. Ito, T. N. Murakami, P. Comte, P. Liska, C. Grätzel, M. K. Nazeeruddin and M. Grätzel, *Thin Solid Films*, 2008, **516,** 4613-4619.
37 T. Fukushima, A. Kosaka, Y. Ishimura, T. Yamamoto, T. Takigawa, N. Ishii and T. Aida, *Science*, 2003, **300**, 2072-2074.
38 T. Merkel, B. Freeman, R. Spontak, Z. He, I. Pinnau, P. Meakin and A. Hill, *Science*, 2002, **296**, 519-522.
39 M. Wang, A. Anghel, B. Marsan, N. Ha, N. Pootrakulchote, S. Zakeeruddin and M. Grätzel, *J Am Chem Soc,* 2009,**131**, 15976-15977.
40 N.-G. Park, J. Van de Lagemaat and A. Frank, *The Journal of Physical Chemistry B*, 2000, **104**, 8989-8994.
41 Q. Wang, J.-E. Moser and M. Grätzel, *The Journal of Physical Chemistry B*, 2005, **109**, 14945-14953.
42 Y. Geng, Y. Shi, L. Wang, B. Ma, R. Gao, Y. Zhu, H. Dong and Y. Qiu, *Phys Chem Chem Phys*, 2011, **13**, 2417-2421.
43 S. J. Lim, Y. S. Kang and D.-W. Kim, *Electrochim Acta*, 2011, **56**, 2031-2035.
44 Y. Wang, J. Zhang, X. Cui, P. Yang and J. Zeng, *Electrochim. Acta,* 2013, **112**, 247-251.
45 S. Sharma, O. K. Varghese, G. K. Mor, T. J. LaTempa, N. K. Allam and C. A. Grimes, *J Mater Chem*, 2009, **19**, 3895-3898.
46 F. Fabregat-Santiago, J. Bisquert, G. Garcia-Belmonte, G Boschloo and A. Hagfeldt, *Solar Energy Materials and Solar Cells,* 2005, **87**, 117-131.
47 W. Zhang, C. Yuan, J. Guo, L. Qiu, F. Yan, *ACS Appl Mater Interfaces,* 2014, **6**, 8723−8728.
48 X. Chen, J. Zhao, J. Zhang, L. Qiu, D. Xu, H. Zhang, X. Han, B. Sun, G. Fu, Y. Zhang and F. Yan, *J Mater Chem,* 2012, **22**, 18018–18024.
49 P. Wang, S. M. Zakeeruddin, J. E. Moser, M. K. Nazeeruddin, T. Sekiguchi and M. Grätzel, *Nat Mater*, 2003, **2***,* 402–407.